Climatic Change (2019) 155:59–79
https://doi.org/10.1007/s10584-019-02444-3

A multi-temporal analysis of streamflow using multiple CMIP5 GCMs in the Upper Ayerawaddy Basin, Myanmar

Uttam Ghimire[1,2] **· Mukand S. Babel**[1] **· Sangam Shrestha**[1] **· Govindarajalu Srinivasan**[2]

Received: 20 July 2018 / Accepted: 16 April 2019 / Published online: 9 May 2019
© Springer Nature B.V. 2019

Abstract
In this study, bias-corrected daily rainfall data of eight global climate models (GCMs) was used as input for a hydrologic model (Hydrological Engineering Center - Hydrological Modeling System (HEC-HMS)) to simulate daily streamflow in the Upper Ayerawaddy River basin (UARB), Myanmar. Monthly, seasonal, annual, and decadal mean flows, calculated for the baseline (1975–2014), were compared with projections for future periods (2040s: 2021–2060 and 2080s: 2061–2100) under two Representative Concentration Pathways (RCP 4.5 and RCP 8.5). The spread of low flows (10th and 25th percentile of daily flows) and high flows (75th, 90th, and 100th percentiles) were analyzed for each period. The ensemble of GCMs indicates an increase in mean monthly (except in October and November), seasonal (except post-monsoon), annual, and decadal rainfalls and corresponding flows in the UARB. Future low flows are expected to have high variability while high flows are expected to have higher means than that of baseline. The density distribution analysis of baseline and future flows reveals that future periods are likely to experience an increase in the magnitude of mean flows but a decrease in variability. Rainfall extremes indicated by 1-day maximum rainfall, 5-day consecutive maximum rainfall, and the number of extreme rainfall days reveals frequent wetter extremes in the UARB under future climate conditions. Extreme floods, as estimated by the frequency analysis of daily flows, are also expected to become more frequent during the future periods. These changes in flows can be attributed solely to climate change since the analyses did not account impacts of possible land use change and water resources development in the UARB. This study is a good starting point to assess future flows, and further research is recommended to address the limitations of this study for improved understanding and assessments that will prove useful for planning purposes in the study area.

Keywords Multi-temporal analysis · Ensemble · Climate models · Streamflow · Ayerawaddy River basin

Electronic supplementary material The online version of this article (https://doi.org/10.1007/s10584-019-02444-3) contains supplementary material, which is available to authorized users.

✉ Mukand S. Babel
msbabel@ait.asia

Extended author information available on the last page of the article

1 Introduction

It is a well-established fact that climate change, driven by greenhouse gas emissions, has intensified significantly in the recent decades (1970–2010) and is likely to increase in the future as well (IPCC 2014). The potential changes in mean climate also alter the frequency and distribution of extreme climatic events and cause stress to hydrological regimes and water resources (Easterling et al. 2000; IPCC 2014; O'Gorman 2015). In several recent studies, CMIP5 (Coupled Model Inter-comparison Project Phase V) global climate model (GCM) outputs have been used as input for hydrological models to assess the impacts of climate change on hydrological processes at the basin scale (Gosain et al. 2006; Krysanova et al. 2017; Shrestha and Htut 2016). Such integration is used to assess the impacts of climate change on water resources and ultimately to aid better planning and operational management of water resources, environmental protection, ecological balance, and so on (Nan et al. 2011).

Myanmar was the world's second most vulnerable country in terms of risks due to extreme weather events between 1994 and 2013 (Kreft et al. 2014). ADB (2009) has also identified it as one of the most vulnerable to climate change, among the countries of Asia and the Pacific. Climate change in Myanmar is expected to impact the country's hydrology and water resources system, agriculture, and human health and settlement. The agriculture sector in Myanmar consumes 90% of the total available water, employs 60% of the country's total labor force, and contributes 22% to the nation's GDP (FAO 2016; IWMI 2019). Hydropower generation also has the potential for economic contribution to the GDP of Myanmar (Kattelus et al. 2015). Frequent hydrological and meteorological extremes like floods and droughts have impacted the lives and livelihoods of many people in Myanmar. Aspects like agriculture, hydropower, and even hydro-meteorological disasters are affected by rainfall and streamflow and are, therefore, closely related to climate change. Thus, an assessment of the impacts of climate change on rainfall and streamflow is required for better climate adaptation plans for any country (Boori et al. 2017; Mendelsohn et al. 2006), and Myanmar most certainly.

Literature about extreme rainfall events in Myanmar is sparse; and yet, there are enough contradictions with respect to the subject. While Endo et al. (2009) reported positive trends in extreme rainfall, Yazid (2015) pointed out negative trends for the same in the northern parts of the country. A recent rainfall analysis of 37 stations revealed wetter yet insignificant trends for total rainfall and extreme rainfall indices during 1981–2015 (Sein et al. 2018). With some yet inconclusive assessments of historical rainfall means and extremes for Myanmar, the projections for future rainfall are even more limited. A few studies indicate an increase in monsoonal rainfalls for all of Myanmar under various climate change scenarios, and only a handful among them have zoomed into basin level projections (Charan Pattnayak et al. 2015; Horton et al. 2016). Only the Bago and Mytinge River Basins have been assessed for potential changes in streamflow under climate change conditions (Khaing 2015; Shrestha and Htut 2016).

Most of the land area under cultivation in Myanmar lies within the Ayerawaddy River basin, and is likely to expand further into the upper parts of the country (Soe 2018). The Upper Ayerawaddy also has the second highest surface water potential among all the river basins in the country (WEPA 2005). The Lower Ayerawaddy and the delta regions of the country often get flooded due to the Upper Ayeyarwady (Kar et al. 2011). Hence, the Upper Ayerawaddy Basin is a promising case study to assess the impacts of climate change on rainfall and streamflow for future periods.

Hydrologic Engineering Center-Hydrologic Modeling System (HEC-HMS) is a hydrological model which has been used extensively for flow simulation under different scenarios of climate and land use changes in river basins across the world including the Mekong and its tributaries in Southeast Asia (Sok and Oeurng 2016; Van Ty et al. 2012). It is a relatively simple model, easy to set up, and demands lesser data than other distributed hydrological models. Daily rainfall data and potential evapotranspiration at monthly resolutions are the minimum data required to set up the model when data is scarce, as is the case in Myanmar.

The key objective of this study was to assess possible changes in the rainfall and streamflow of the Upper Ayerawaddy River basin (UARB), located in northernmost part of Myanmar, at multiple temporal resolutions (monthly, seasonal, annual, decadal), and low (Q5 and Q25) and high (Q75 and Q90) flows, under RCPs 4.5 and 8.5, using eight CMIP5 GCMs so as to provide evidence-based changes in mean and extreme rainfall events and river flows under climate change conditions. This study is the first of its kind in the UARB. The inclusion of possible land use changes and water resources development in the analysis was beyond the scope of the current study; these inclusions are for future research so that the analysis can be made more extensive for water resources planning in the study area.

2 Materials and methods

2.1 Study area

The major drainage system of Myanmar is the Ayerawaddy River, which flows north to south and drains 66% of the total area of the country (~ 676,600 km^2) into the Andaman Sea (Brakenridge et al. 2017). This river is further divided into Chindwin (985 km), and Upper (1039 km) and Lower Ayerawaddy Rivers (680 km). Figure 1 shows the location map of the Ayerawaddy River basin in Southeast Asia, the study area (Upper Ayerawaddy River basin: UARB), and the rainfall and discharge stations used in this study.

The UARB drains an area of 125,000 km^2 (34% of the Ayerawaddy Basin) to a discharge station called Sagaing, which is above the confluence of the Chindwin and the Upper Ayerawaddy rivers (Fig. 1). The elevation in the study area varies from 50 to 5770 m, as per the digital elevation model (DEM) of 90 m resolution accessed from HydroSHEDS for hydrological modeling (Lehner et al. 2006). A land cover map for 2006, obtained from the European Space Agency (ESA), shows that 70% of the study area at that time was covered by forests, 15% by agricultural lands, and 2% by permanent snow and other land use (Defourney et al. 2006).

2.2 Historical and future data

Table 1 summarizes the daily rainfall and discharge data, for six and three stations respectively, collected from the Department of Meteorology and Hydrology (DMH), Myanmar. The locations of these stations in the study area are shown in Fig. 1. Table 1 presents the details of the eight GCMs selected for projections of rainfall for the future periods relevant to this study.

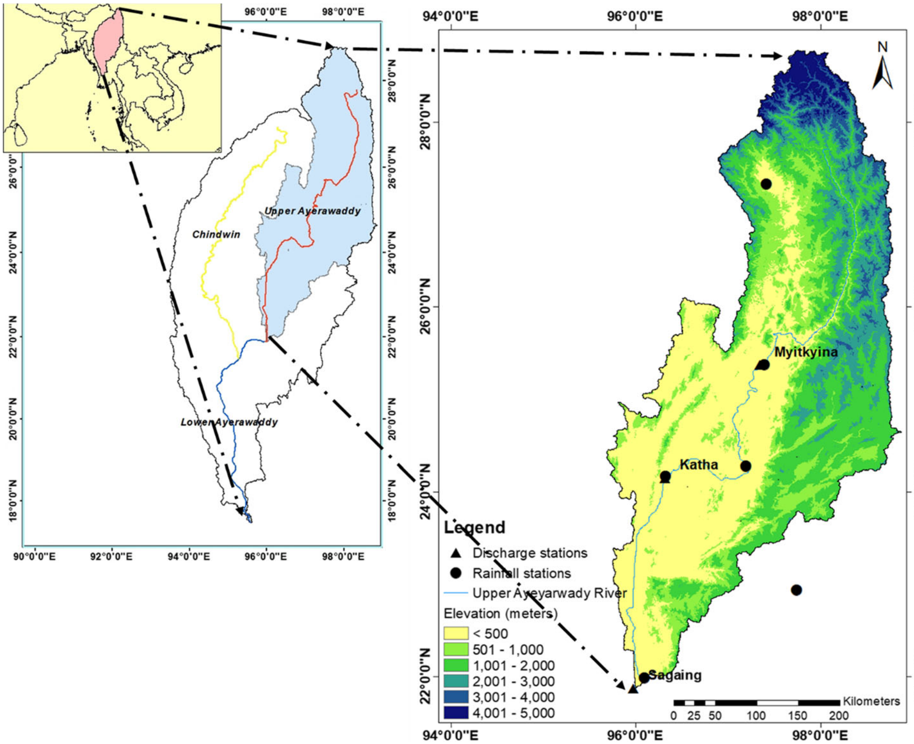

Fig. 1 Location map of the study area, rainfall, and discharge stations considered for the study

2.3 Methodology

2.3.1 Rainfall bias correction

The quantile mapping technique was used at a daily time step to reduce the biases of GCM rainfall data at the station level. This technique was chosen for this study because, in the past, it has performed better than the linear scale method of bias correction for the study area (Ghimire 2016). The "Qmap" package available in R was used in this study to map the quantiles of GCMs with those of observed rainfall at daily time step (Gudmundsson et al. 2012). A control period of 1975–2005 was selected to compare and map observed and GCM rainfall. Two periods, of 40 years each, were identified for the future—2021–2060 (the 2040s) and 2061–2100 (the 2080s)—to maintain consistency with the baseline duration (1975–2014) and for frequency analysis in case more than 30 years of data was required.

2.3.2 Analysis of projected rainfall

Bias-corrected GCM rainfalls for the future periods of the 2040s and 2080s were compared with the baseline at a monthly timescale to understand the changes in rainfall and the variability projected by GCMs at station and basin scales. The trends of projected rainfall for the study area were computed using Sen's slope method (Sen 1968) and checked for their significance at 5% using the non-parametric Mann–Kendall test (Kendall 1955; Mann 1945).

Table 1 Rainfall and discharge stations and the GCMs used in this research

Rainfall stations (1975–2014)					
Station	Latitude (°)	Longitude (°)	Elevation (m, MSL)	Mean annual rainfall (mm)	Std. dev (mm)
Putao	27.3	97.4	409	4032	644
Myitkyina	25.4	97.4	145	2244	334
Bhamo	24.2	97.2	111	1846	304
Katha	24.1	96.3	94	1543	308
Lashio	22.9	97.7	856	1277	169
Mandalay	21.9	96.1	93	850	253
Discharge stations (2000–2014)					
Station (area (km^2))	Latitude (°)	Longitude (°)	Elevation (m, MSL)	Mean flow (m^3/s)	Specific discharge (m^3/s/km^2)
Myitkyina (48,973)	25.4	97.4	145	4667	0.095
Katha (84,273)	24.2	96.3	94	5028	0.060
Sagaing (124,857)	21.9	96.0	64	5878	0.047
Global climate models (GCMs); RCP 4.5 and RCP 8.5					
Model	Resolution (lat (°)×long (°))		Research center	Vintage	
BCC-CSM1–1	2.78×2.81		BCC, China	2011	
CCSM4	0.94×1.25		NCAR, USA	2010	
CNRM-CM5	1.40×1.40		CNRM & CERFACS	2010	
CSIRO-Mk3–6-0	1.85×1.87		CSIRO, Australia	2009	
IPSL-CM5A-MR	1.27×2.50		IPSL, France	2009	
MIROC5	1.40×1.40		MIROC, Japan	2010	
MPI-ESM-LR	1.85×1.87		MPI, Germany	2009	
MRI-CGCM3	1.11×1.12		MRI, Japan	2011	

A similar analysis was done for the baseline period (1975–2014) using mean rainfall computed from the interpolated weights of six meteorological stations. Such analysis for the baseline period improves the understanding of trends of projected rainfall in a basin.

One-day maximum rainfall (Rx1day), 5-day consecutive maximum rainfall (Rx5day), the number of days with moderate rainfall (R10, rainfall rate more than 10 mm/day), and the number of days with extreme rainfall (R30, rainfall rate more than 30 mm/day) were considered as rainfall extreme indices in this research. Such indices were estimated at the basin level for future periods using an ensemble of climate models and were compared for their deterministic exceedance frequencies against the baseline period. Trends of these indices at the basin level were also analyzed using techniques like those used for mean rainfall.

2.3.3 Hydrological model setup using HEC-HMS

Four sub-basins were delineated in the UARB to set up a hydrological model using HEC-HMS. The SCS curve number method was used to compute effective rainfall for each sub-basin, which was transformed into streamflow using the SCS unit hydrograph. Linear reservoir and constant monthly base flows were assigned to the sub-basins to account for low flows in the study area. The flows generated at the sub-basin outlets were routed using the lag and Muskingum methods. Constant monthly evapotranspiration was considered to account for losses in the basin. No snowmelt was considered in the modeling.

Calibration and validation periods of 2000–2008 and 2009–2013, respectively, were used to assess the hydrological model's ability to represent the rainfall-runoff processes in the study area on a daily time scale. The univariate gradient method was used to auto-optimize the basin's parameters during the calibration process. The hydrological model was tested for its performance using several indicators like the coefficient of determination (R^2), the average normalized peak error (ANPE), the ratio of root mean square error (RMSE) to standard deviation (RSR), Nash–Sutcliffe efficiency (NSE), and percentage bias (BIAS %) (Krause et al. 2005; Moriasi et al. 2007; Sun et al. 2000).

To analyze the impacts of rainfall on streamflow in the future in the UARB, bias-corrected GCM rainfall for the future periods was used as input in the developed model, and flows were simulated. Expected land use changes and water resources development in the future periods were not considered in this analysis.

2.3.4 Uncertainty analysis

Uncertainties in projections of future flows can arise from several factors including different GCMs and their inherent characteristics, the choice of emission scenarios, downscaling/bias correction techniques, and the choice of hydrological models (Prudhomme and Davies 2009; Wilby and Harris 2006). It has often been found that the selection of GCMs is responsible for the most amount of uncertainty, much more than the uncertainty arising from emission scenarios, downscaling techniques, and hydrological models (Kay et al. 2009; Prudhomme and Davies 2009; Wilby and Harris 2006). The uncertainties in flows arising from hydrological models have been found to be the lowest among other sources of uncertainty for mean and low flows (Q10) for 12 large river basins, including the Ganges, across the world (Vetter et al. 2017).

The two-way analysis of variance (ANOVA) method can be employed to quantify the sources of uncertainty in rainfall and temperature projections while a three-way ANOVA method can be used for flow projections (Aryal et al. 2018; Vetter et al. 2017). In this study, uncertainty in projected flow arose only from the selected GCMs and emission scenarios (ES RCP 4.5 and RCP 8.5) as bias correction (quantile mapping) and hydrological modeling (HEC-HMS model) were done through the same method. In this study, a two-way ANOVA method conducted using the SPSS software to analyze the interaction between GCMs and ES while predicting flows is defined as:

$$\mathrm{SST} = \mathrm{SS}_{(\mathrm{GCM})} + \mathrm{SS}_{(\mathrm{ES})} + \mathrm{SS}_{(\mathrm{GCM*ES})}$$

where SST = total sum of squares, $\mathrm{SS}_{(\mathrm{GCM})}$ = sum of squares due to climate models, $\mathrm{SS}_{(\mathrm{ES})}$ = sum of squares due to emission scenarios, and $\mathrm{SS}_{(\mathrm{GCM*ES})}$ = sum of squares due to the interaction between climate models and emission scenarios.

2.3.5 Analysis of flows at multi-temporal scales

The mean flows simulated for the future periods of the 2040s and 2080s were compared with the baseline flow at monthly, seasonal, annual, and decadal scales. Mean monthly flows during the 2040s and 2080s simulated by the ensemble of climate models were assessed for changes (in percentage) with respect to mean monthly baseline flows. Annual flows simulated by the ensemble of climate models for the period of 2021–2100 were compared with mean annual baseline flows for both scenarios of climate change. The five seasons that Myanmar experiences—pre-monsoon (mid-April to mid-May), monsoon (mid-May to mid-October), post-monsoon (mid-October to end-November), dry and cool seasons (end-November to mid-March), and hot season (mid-March to mid-April)—were considered in this research (Htway and Matsumoto 2011). Mean seasonal flows during the 2040s and 2080s, as simulated by the ensemble of climate models, were also compared with mean seasonal flow of the baseline period.

The decades for this research were defined as 2021–2030, 2031–2040, and so on. Mean decadal flows simulated by the ensemble of climate models were compared with mean flow during the baseline period. The inter-decadal variability of the means of flows as simulated by the climate models was also computed for each decade.

2.3.6 Analysis of flow extremes

Low flows (represented as 10th and 25th), median flows (50th), high flows (75th and 90th), and annual maximum flows (100th) percentile of the daily flows were computed for the 2040s and the 2080s and compared with the baseline values. Trend analysis of low (Q10), median (Q50), and high (Q90) flows was done for the baseline period (1975–2014) using the rainfall simulated flows and for the projected periods using GCM-simulated rainfall flows. These trends were also computed using Sen's slope method (Sen 1968) and checked for their significance at 5% level using the non-parametric Mann–Kendall test (Kendall 1955; Mann 1945).

Density distribution of Q50 (median) and annual maximum flows (Q100) during the baseline and future frames were fitted with normal and Gumbel distributions respectively and tested for the goodness of fit using the Kolmogorov–Smirnov test at 1, 5, and 10% significance levels. These distributions and testing techniques have been used extensively for flow and flood frequency analysis in several regions of the world (Garba et al. 2013; Yue et al. 1999). The annual maximum flows were then analyzed for their frequencies during the baseline period and projected future periods of the 2040s and 2080s using the mean of flows as simulated by the ensemble of climate models.

3 Results and discussion

3.1 Bias correction of rainfall

The period of 1975–2005 was used to estimate rainfall bias correction factors using the quantile mapping technique for the individual GCMs which were selected for this study. Overall, GCMs at the station level mostly underestimated rainfall in the upper part and overestimated it in the lower part of the UARB, as compared to the observed rainfall data. Figure 2 (top row) shows the mean monthly comparison of GCMs before and after bias correction with the observed rainfall at the Myitkyina station for 1975–2005.

After quantile mapping, the GCM rainfall data at daily resolution, the GCM monthly aggregated data and observed rainfall data at the station level matched well, as can be seen in Fig. 2 for Myitkyina. The effects of quantile mapping on daily GCM data have not been discussed in this study, though the lower quantiles (less than 10%) were over-fitted while higher quantiles (more than 90%) were over-estimated; this has been discussed as the limitations of quantile mapping (Maraun 2013).

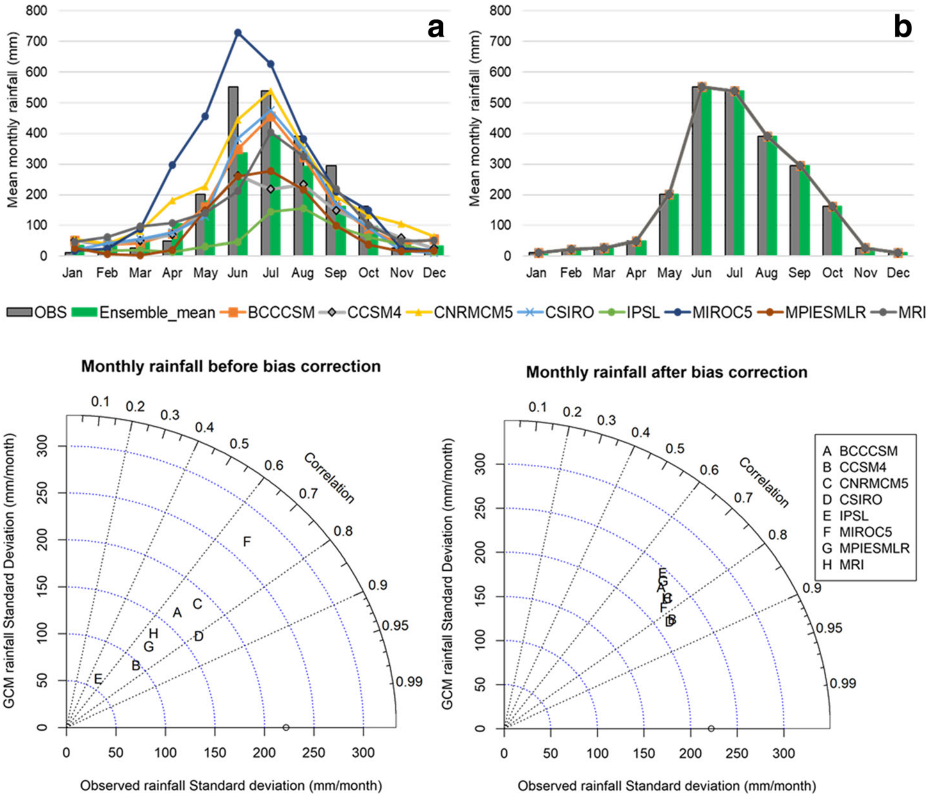

Fig. 2 Observed and GCM-simulated mean monthly rainfall during 1975–2005 at Myitkyina before (**a**) and after (**b**) bias correction

3.2 Projected changes in rainfall

Mean rainfall in the basin is projected to experience a significant increase during April–June and is expected to decrease during September–November under the selected climate change scenarios (Fig. 3). The standard deviation of changes simulated by the eight climate models, presented as error bars for each month, shows higher spread during May and June. It was also observed that while most of the GCMs are unidirectional in projecting mean monthly changes during September to May, for the remaining months, they do not project a clear trend of change in rainfall.

It was seen that while net changes are higher during high rainfall months, relative changes are likely to be higher during the months of low rainfall (November to March). The highest mean changes and greater variability among GCMs in simulating mean basin rainfall is expected for the 2080s. The upper part of the basin is expected to experience more changes as compared to the lower part, as is also represented by the projected rainfall at the selected stations (Supplementary Fig. A).

A significant increasing trend of 8.15 mm/year was observed for annual rainfall over the basin during the baseline period (Supplementary Fig. B). However, majority of the selected future periods and RCP scenarios did not show any significant trends of mean annual rainfall

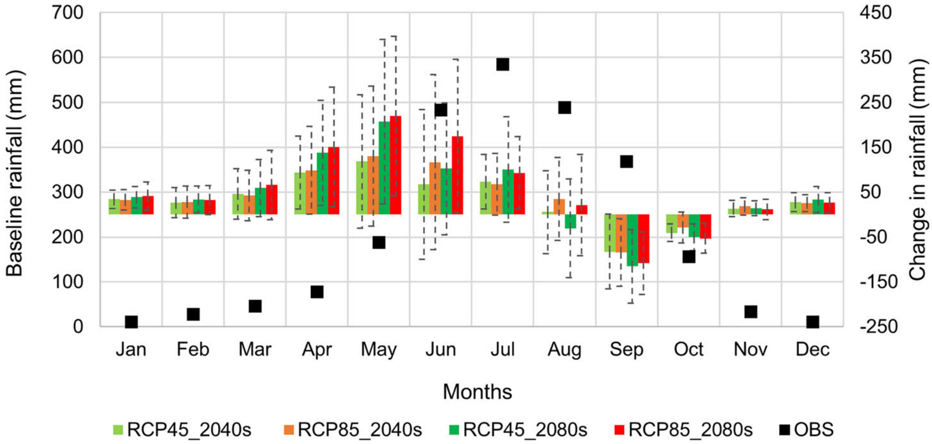

Fig. 3 Baseline (OBS) mean monthly rainfall for the basin and projected mean changes and variabilities expressed as standard deviation for RCP 4.5 and 8.5 during the 2040s and 2080s

in the UARB. In general, upon comparing the mean of all GCMs to the baseline data, mean annual rainfall for the study area is projected to increase by 16–20% during the 2040s and 21–28% during the 2080s. Similar increases, in the range of 6–23% (as compared with the baseline period of 1980–2006) for mean annual rainfall, have been reported for all of Myanmar for 2041–2070 (Horton et al. 2016).

Despite insignificant trends of Rx1day and Rx5day during the baseline period, these two indices show an increase in rainfall extremes under both climate change scenarios. All the GCMs were found to be unidirectional in projecting the increase in the frequencies of these two indices for the 2040s and the 2080s (Fig. 4).

Increased frequencies of Rx1day in the study area under the selected climate change scenarios imply frequent occurrence of disasters like landslides and flash floods. An example of such a disaster in the UARB was 80 mm of rainfall on 21 June 2018 at the Myitkyina station, which led to a massive landslide in Hpakant (100 km from the station), killing more than a hundred people (Davies 2018). Rx5day, which contributes more towards riverine flooding, is also projected to become more frequent in the study area in the future.

Moderate rainfall days (R10), which had a significant increasing trend of 0.33 days/year during the baseline period, are expected to decrease during the future periods (Fig. 5**a**–**d**). For example, the UARB had at least 60% probability that there would be 100 days with rainfall more than 10 mm during the baseline period; this probability reduces to 20–30% under RCP 4.5 and 30–40% under RCP 8.5. Disagreement among GCMs was also observed in the projection of R10, with many of the models pointing to a decrease in moderate rainfall days. However, R30, with insignificant trends during the baseline period, is expected to distinctly increase extreme rainfall days during the future periods (Fig. 5**e**–**h**). This decrease of R10 and increase of R30 indicate that the UARB is likely to receive more extreme rainfall days and increased rainfall intensity under the selected climate change scenarios. A very good agreement was observed among GCMs in projecting R30 for the UARB, as has been visualized by the thin ensemble band of the GCMs' R30s for the future periods (Fig. 5**e**–**h**).

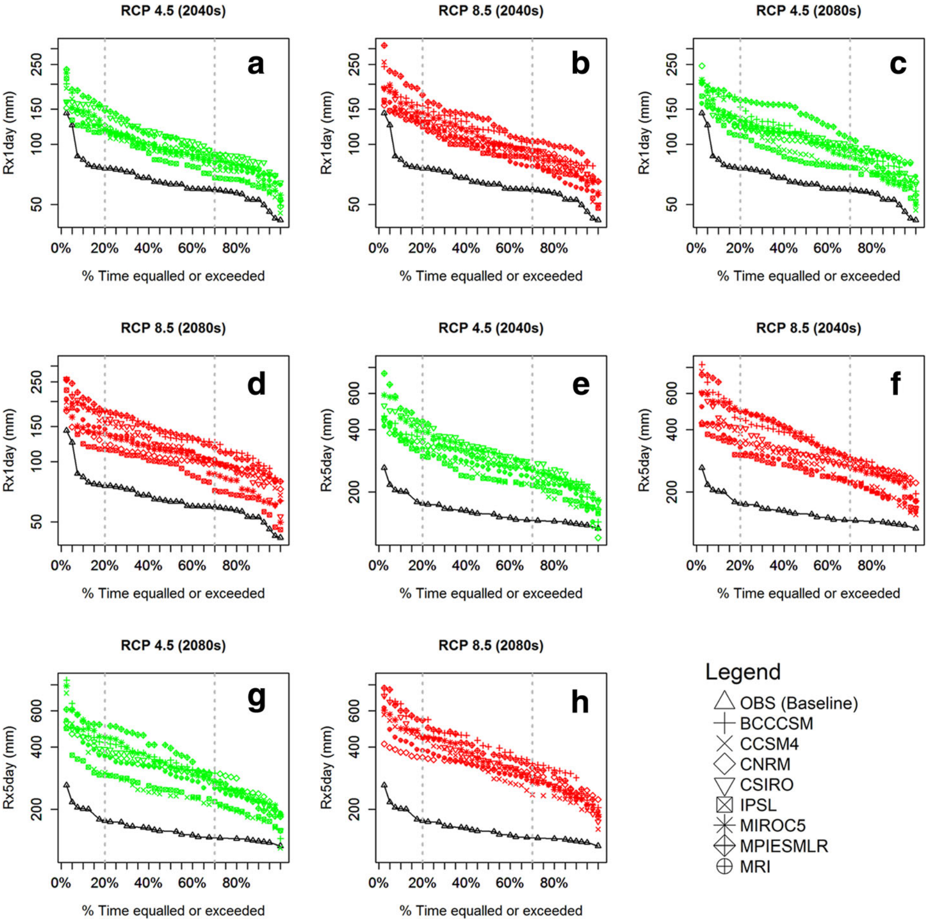

Fig. 4 Deterministic frequency duration curves computed for Rx1day (**a**–**d**) and Rx5day (**e**–**h**) for the baseline period, and under RCP 4.5 and RCP 8.5 during the 2040s and 2080s

3.3 Calibration of the hydrological model

Figure 6 presents the calibrated sub-basin parameters, sub-basin elements, and the sensitivity analysis of the model's parameters in the UARB.

A total of 500 iterations were used with a tolerance of 0.01 for calibration at each of the three hydrological stations to optimize the basin's parameters. Based on the volume of flow, the groundwater parameters were found to be the most sensitive among all the chosen parameters.

The finalization of the hydrological model's parameters during the calibration period of 2000–2008 was tested over an independent validation period of 2009–2013. The model's performance statistics indicate that the HEC-HMS model could represent the rainfall runoff processes of the study area at a daily time step very well (Fig. 7).

Based on the hydrological model evaluation criteria of Moriasi et al. (2007), the calibrated model was found to be satisfactory at Myitkyina and very good at the Katha and Sagaing discharge stations.

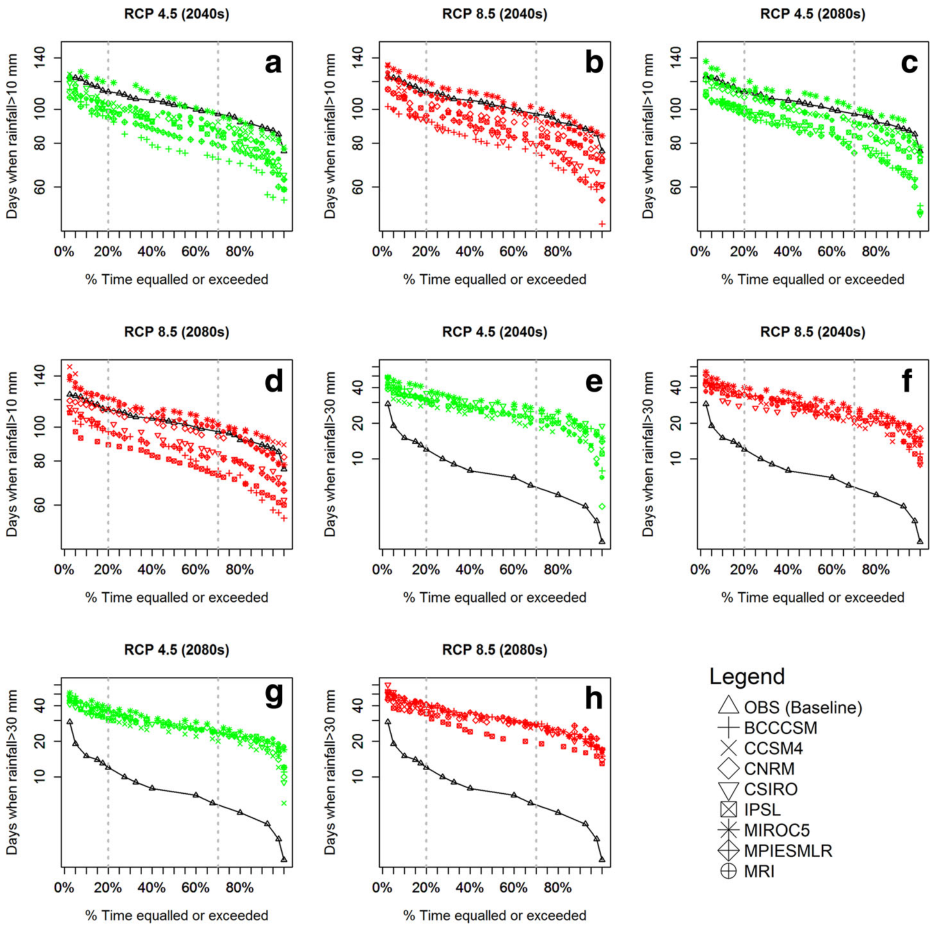

Fig. 5 Deterministic frequency duration curves computed for R10 (**a**–**d**) and R30 (**e**–**h**) for the baseline period and RCPs 4.5 and 8.5 during the 2040s and 2080s

Improvements in performance indicators were observed for GCM simulated flows after the GCM rainfall data was bias corrected and fed into the developed hydrological model. A comparison of monthly flows computed using daily simulation during 1975–2005 revealed that bias corrected GCM rainfall could yield satisfactory results in the study area (Supplementary Fig. C).

3.4 Analysis of uncertainty in predicted flows

The fraction of variance (SST) was used to show the contribution of each source of uncertainty in flow simulation for the study area. During all the months of the future periods, GCMs contributed maximum uncertainty, as reflected by the higher values of the fraction of variance. The interaction between GCMs and the scenarios caused lesser uncertainty than GCMs alone, and the scenarios by themselves were responsible for even less uncertainty (Fig. 8).

Calibrated Sub-basin parameters

SCS Loss method				
Parameters	W350	W440	W640	W660
Initial abstraction (mm)	50	30	23	30
Curve Number	78	75	70	70
Impervious (%)	10	20	22	20

SCS UH Transform				
Parameters	W350	W440	W640	W660
Graph Type	Delmarva	Delmarva	Delmarva	Delmarva
Lag time (min)	7000	20000	9000	6000

Routing: Lag method	
Parameter	R600
Lag time (min)	6000

Baseflow: Constant monthly method			
Parameters	W440	W640	W660
Monthly Q (m3/s)	300	200	100

Baseflow: Linear reservoir method (W350 Subbasin)			
GW1 Initial (m3/s)	1384	GW2 Initial (m3/s)	300
GW1 Coefficient	1500	GW2 Coefficient	20
GW1 reservoirs	45	GW2 reservoirs	11

Routing: Muskingum method		
Parameters	R630	R250
Muskingum K (HR)	24	24
Muskingum X	0.3	0.3
Num. of Subreaches	3	3

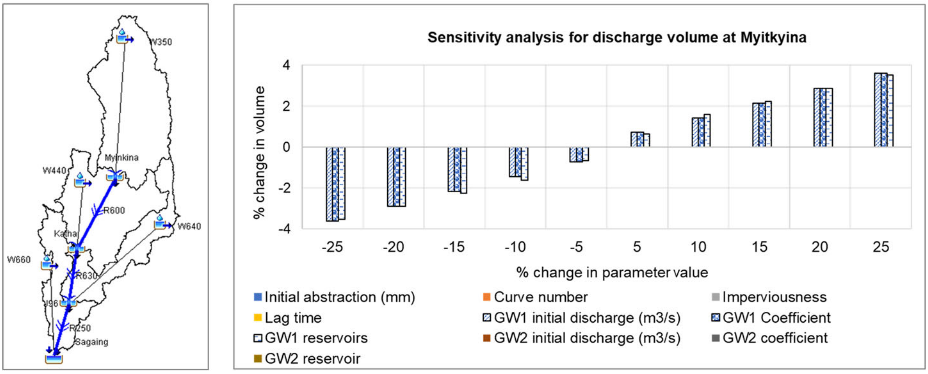

Fig. 6 Calibrated sub-basin parameters, sub-basin elements, and sensitivity analysis for discharge volume at the Myitkyina hydrological station

During the 2040s, the combined uncertainty due to GCMs and scenarios is significant (20–40%) in August and September; while during the 2080s, this uncertainty is less than 20% in all the months. Thus, the streamflow projections are presented as the ensemble and mean of ensembled flows simulated by the selected eight GCMs, as it was clear that GCMs are largest source of uncertainty in this study.

3.5 Projected multi-temporal flows

Mean flows are projected to experience significant relative increase during the non-monsoonal months and decrease in October and November during both future periods (Fig. 9 top row), as compared with the baseline period. Mean monthly changes ranging from − 11 to 85% in the 2040s and − 7 to 80% in the 2080s are predicted under RCP 4.5 in the UARB. Similarly, under RCP 8.5, these changes, computed using the mean of flows simulated by an ensemble of climate models, are expected to be in the range of − 20 to 108% during the 2040s and − 17 to 109% during the 2080s.

The projected variability in mean monthly flows is higher under RCP 8.5 than under RCP 4.5. Higher relative increases are projected for the low flow months of January to April. Peak flow months of the baseline period, June to September, are projected to experience an increase of less than 50% while the months of October and November are

Myitkyina (Daily flows)		
Indicator	**Calibration**	**Validation**
R^2	0.72	0.76
ANPE	0.14	0.13
RSR	0.69	0.7
NSE	0.53	0.5
BIAS (%)	3.84	17.23
Performance	Satisfactory	Satisfactory

Katha (Daily flows)		
Indicator	**Calibration**	**Validation**
R^2	0.84	0.86
ANPE	0.07	0.11
RSR	0.45	0.54
NSE	0.79	0.71
BIAS (%)	7.17	18.77
Performance	Very good	Good

Sagaing (Daily flows)		
Indicator	**Calibration**	**Validation**
R^2	0.81	0.81
ANPE	0.08	0.09
RSR	0.49	0.48
NSE	0.75	0.77
BIAS (%)	8.78	6.97
Performance	Very good	Very good

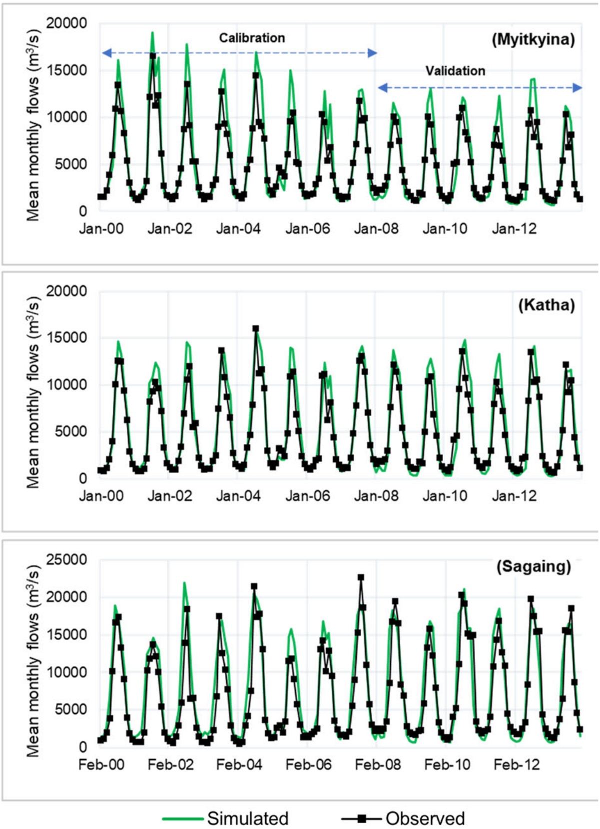

Fig. 7 Hydrological model performance indicators computed using daily flows and monthly plots of observed and rainfall simulated flows derived during the calibration and validation periods at the Myitkyina (top-most), Katha (middle), and Sagaing (bottom) flow stations

projected to experience a decrease of less than 25% under both scenarios. These changes in mean monthly flows throughout the future periods are also translated as changes in mean flows for dry and cool, hot, pre-monsoon, monsoon, and post-monsoon seasons in the study area (Fig. 9 middle row).

Baseline dry and cool seasonal flows of 1575 m^3/s are expected to increase in general by 1000 m^3/s with less variability than other seasons, during the future periods. Mean hot seasonal flows of 1931 m^3/s during the baseline are projected to increase to 3412 m^3/s (3406 m^3/s) and 3926 m^3/s (4009 m^3/s) under RCP 4.5 (RCP 8.5) scenario during the 2040s and 2080s respectively. Monsoonal flows are also expected to increase by 3007 m^3/s (3590 m^3/s) and 3761 m^3/s (4910 m^3/s) under RCP 4.5 (RCP 8.5) scenario during the 2040s and 2080s respectively. Similarly, post-monsoonal flows are expected to decrease by 10.4% (5.6%) during 2040s, and by 16.3% (14.8%) during 2080s under the RCP 4.5 (RCP 8.5) scenario of climate change.

The Nam Ou river basin in Lao PDR also yielded higher relative changes in flows during the non-monsoonal months (up to 105% increase as compared with the baseline) and higher net changes during monsoonal months (baseline of 15,000 m^3/s increased up to 30,000 m^3/s) when a multi-model ensemble was used for future projections (Shrestha et al. 2013). Similarly, under various climate change scenarios, the flows in the Bago River Basin, Myanmar are projected to experience 84% increase in summer (baseline is 2 m^3/s, the projected value is 3.2 m^3/s) and 22% increase in the rainy season (net increase of 65 m^3/s) (Shrestha and Htut 2016). This increase in pre-monsoon flows for the study area may change the flow regimes of the Lower Ayerawaddy region where floods are common whenever high rainfall/flows in the Upper Ayerawaddy coincide with high rainfall/flows of the Chindwin Basin; the flooding may even start sooner than now in the future (Kar et al. 2011). However, the agriculturally dominant dry zone area of Myanmar, which is located just downstream of the study area, may opt to grow crops which thrive well in wetter conditions in the future.

The mean annual flows are projected to increase in all future years under both scenarios of climate change (Fig. 9 bottom row). The mean increase in annual flows, as simulated by the mean of ensembled flows of climate models, is 24% (27.8%) during the 2040s and 30.4% (37.4%) during the 2080s under RCP 4.5 (RCP 8.5) scenario. In general, the annual variations are found to be higher under RCP 8.5 scenario, compared with RCP 4.5 during both the periods.

It was observed that all the climate models are unidirectional in pointing towards an increase in mean decadal flows in the UARB during the future scenarios of climate change (Fig. 10).

The variability among decadal mean flows, as simulated by the various climate models, is lesser under RCP 4.5 than under RCP 8.5.The mean baseline decadal flows are projected to increase by 21% during 2021–2030 to 33% by 2091–2100 under RCP 4.5, when the average of the decadal flows, as simulated by the members of the ensemble of the climate models, is considered. Under RCP 8.5, these mean decadal increases are 22.7% and 41.8% for 2021–2030 and 2091–2100 respectively. The inter-decadal variabilities computed for the ensemble's mean of flows in the study area show consistent increase in the median value across the decades under both scenarios. The years between 2021–2030 and 2051–2060 have a variability of 10–47% increase in inter-decadal flows

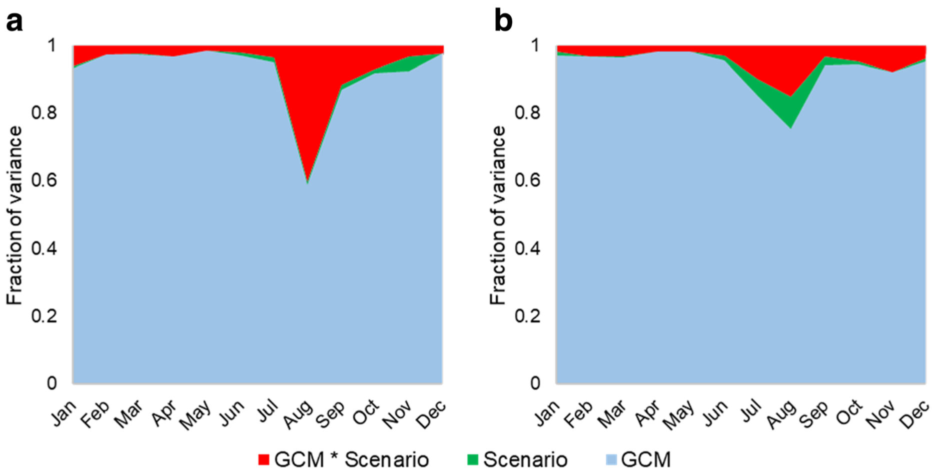

Fig. 8 Contribution of sources of uncertainty represented as fraction of variance during the 2040s (**a**) and 2080s (**b**)

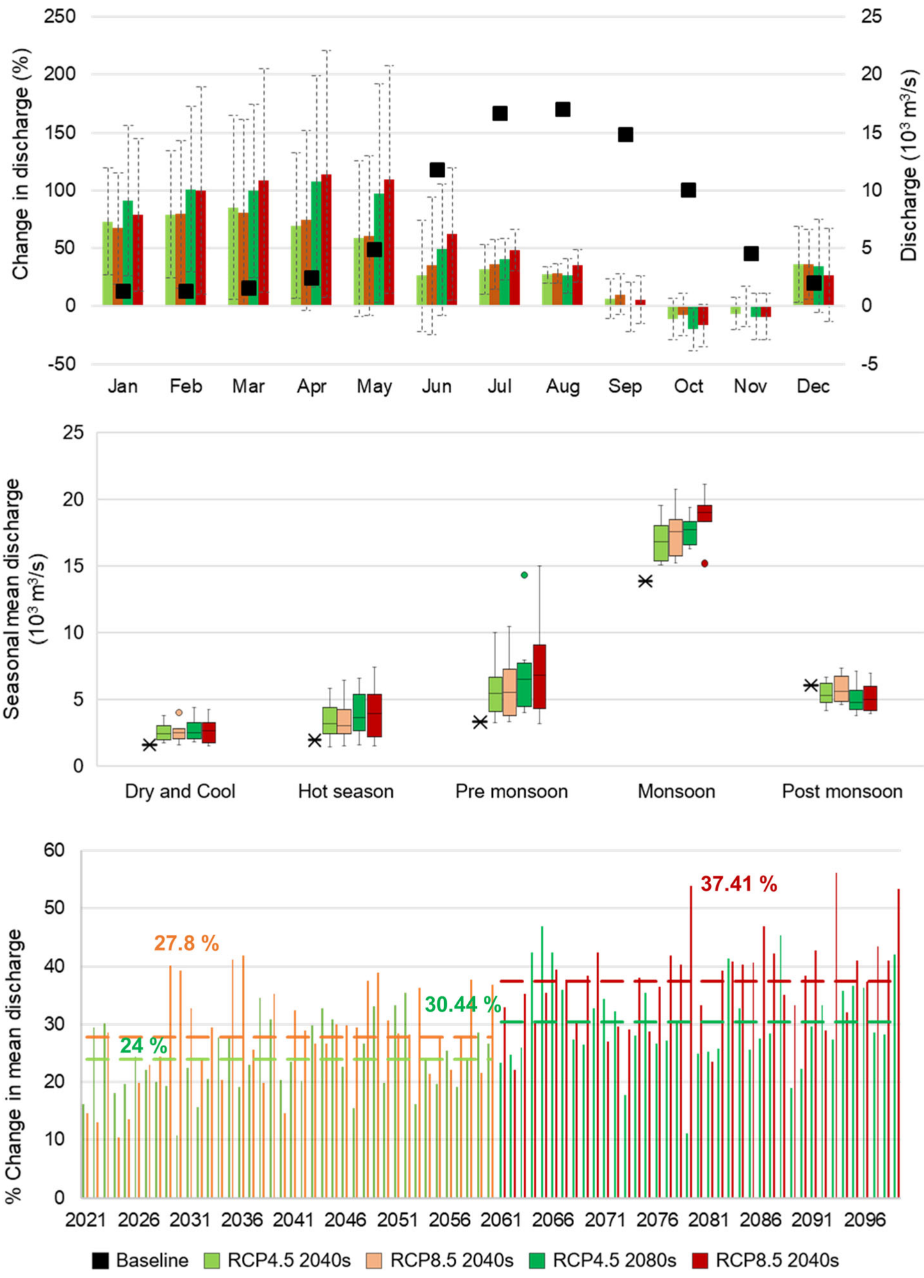

Fig. 9 Baseline mean monthly flows (m^3/s) and projected changes (%) (top figure), baseline and projected mean seasonal flows (m^3/s) (middle figure) and projected changes (%) in annual mean flows at the study basin's outlet (bottom figure) during the 2040s and 2080s under RCP 4.5 and RCP 8.5 simulated by the ensemble mean of climate models

which increases to 11–57% during 2061–2070 to 2091–2100, as compared with the baseline median value.

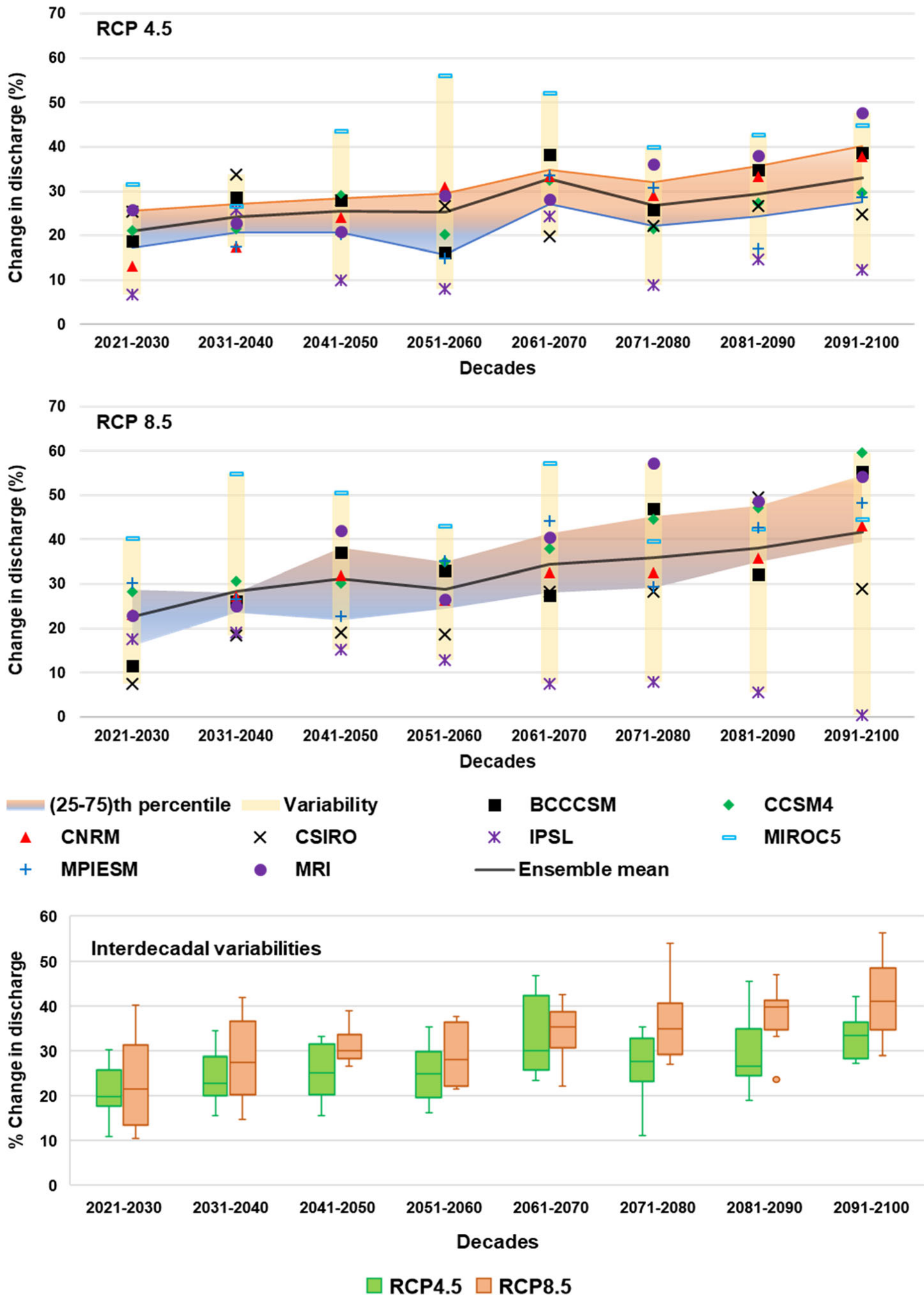

Fig. 10 Changes in mean decadal flows at the Sagaing discharge station as simulated by the ensemble of climate models under RCP 4.5 (top figure) and RCP 8.5 (middle figure), as compared with the baseline and the inter-decadal variabilities in the mean of ensemble flows for RCP 4.5 and RCP 8.5 (bottom figure)

3.6 Changes in extreme flows

A comparison of the normal density distribution of annual flows computed as an average of flows simulated by the ensemble of climate models for the future periods with the normal density distribution of annual flows of the baseline period reveals the increase in magnitude and frequency of annual flows during the future periods (Fig. 11a). The variability is likely to

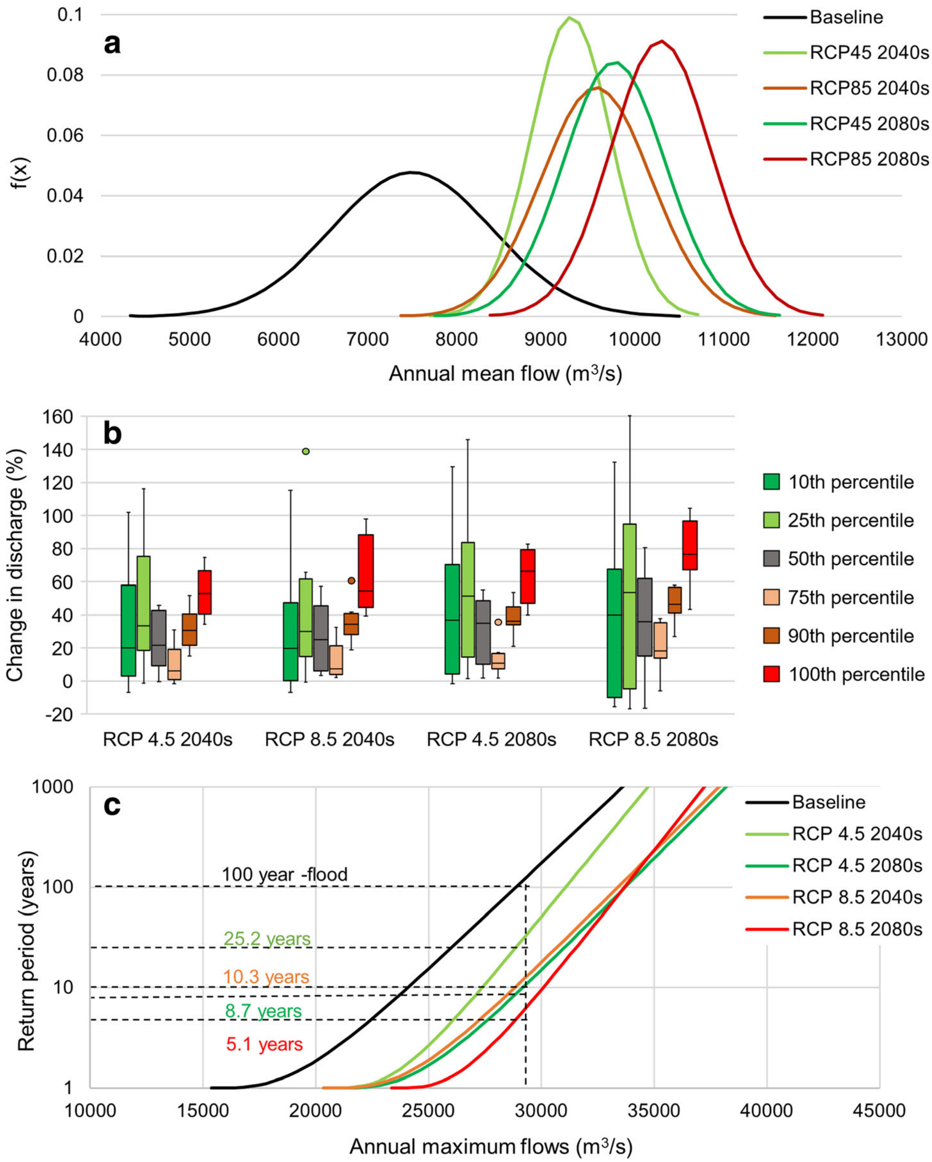

Fig. 11 Probability density functions of baseline annual average flows and projected future flows computed by averaging the flows simulated by the ensemble of climate models (**a**), relative changes (%) in low, mean, and high flows in the future periods compared to the baseline (**b**) and annual maximum flows (m^3/s) and their corresponding return periods (years in log scale) during the baseline and projected future periods (**c**)

reduce in the future, but the shift of the density function towards the right tail indicates that the future years are likely to experience above-normal mean annual flows.

It has been widely discussed that with changes in mean values of climatic variables like precipitation, extreme values represented by the distributional tails are also likely to get affected in a non-proportional ratio to that of the mean (Tebaldi et al. 2006). While the median flow for the study area is projected to experience mild increases in the future periods, low and high flows, represented by respective quantiles of daily flows, are predicted to behave differently (Fig. 11b). The median flow (Q50), which had a significant increasing trend during the baseline period (Supplementary Fig. D), is projected to increase by 20.0% (25.0%) during 2040s and 38.0% (36.0%) during 2080s under the RCP 4.5 (RCP 8.5) scenario. The annual maximum flow (Q100) is projected to experience the highest relative increases during the future periods. The least change in median and variability is seen for the 75th percentile flow, followed by Q90 in the future. Trendless low flows during the baseline period (Supplementary Fig. D) are projected to remain trendless for the future periods as well, with the least median increment and highest variabilities among all other quantiles of flows.

An assessment of 5, 10, 25, 50, and 100-year return period floods of the baseline period revealed that such floods will be frequent in the future (Fig. 11c). Upon inspection, a 5-year return period flood of magnitude 22,538 m^3/s during the baseline is projected to occur yearly under the climate change scenarios. A 10-year return period flood at the Sagaing discharge station is also projected to occur once every 2–3 years in the future. A distinct decrease in 100-year floods up to 5-year is projected during the 2080s under RCP 8.5. Such extreme flows have been projected to become frequent during future periods in Myanmar in other studies also (Boori et al. 2017).

These results indicate that water infrastructures designed and constructed without considering such effects of climate change may be posed serious challenges in the future. A detailed in-depth investigation of the impacts of climate change at a subdaily scale is necessary for more reliable estimates of changes in design discharges. Such investigations should account for uncertainties arising due to climate models, emission scenarios, bias correction techniques, and hydrological models. The results of this study are based only on the possible effects of climate change. However, other driving factors such as land use changes should also be considered before developing suitable remedial and adaptation strategies for the UARB in Myanmar.

4 Summary and conclusions

This study shows that streamflow in the UARB, Myanmar, as simulated by a semi-distributed hydrological model (HEC-HMS), fed with rainfall from eight GCMs, and compared with the baseline (1975–2014) flow at multi-temporal resolutions, is projected to increase in the future. Future time periods of the 2040s (2021–2060) and the 2080s (2061–2100) are expected to experience increases in rainfall and streamflow under both scenarios, but more so under RCP 8.5 than RCP 4.5, as compared with the baseline. Mean monthly rainfall and flows are projected to increase relatively more during December to April and decrease during September to November in the future. All the seasons, except post-monsoon, are projected to experience significant increases in mean rainfall and flows during the future periods with higher relative increases in nonmonsoon seasons and higher net increases during monsoonal seasons. Mean annual rainfall (flows) in the basin is projected to increase by 16–20% (24–27%) during the 2040s and by 21–28% (30.4–37.4%) in the 2080s, when the mean of all GCMs was compared with the baseline data. As expected, the mean decadal flows in the study basin are also projected to increase by 21.0% (22.7%) during 2021–2030, and to 33.0% (41.8%) during 2091–2100 under RCP 4.5 (RCP 8.5) scenario. In general, the annual variations and decadal variabilities in flows were higher for the period of the 2080s under both scenarios in the UARB. The analysis of the distribution of mean flows for the basin under future and baseline periods reveals an increase in the magnitude and frequency of mean flows in the basin. The projected changes in low and high flows were found to be disproportionate to the increase in mean flows. In general, high flows had relatively higher increases in median value over the baseline period while low flows exhibited higher variability for future periods. Rainfall extreme indices like 1-day maximum rainfall, 5-day consecutive maximum rainfall, and the number of rainy days with rainfall rate more than 30 mm/day revealed that the basin is likely to experience wetter extremes in the future. The frequency analysis of annual maximum flows also revealed that extreme flows are projected to become more frequent in the future in the UARB.

5 Limitations and recommendations

While this study employed a standard approach to assess the impacts of climate change on streamflow in the UARB using multiple GCMs, a bias correction scheme and a semi-distributed hydrological model, assessments can be improved by considering impacts of possible land use changes, development of water resources projects like reservoirs and hydropower, and uncertainties associated with future climate scenarios, bias correction methods, and hydrological models. Despite these limitations, this study is a starting point for further research to address these various uncertainties to improve our understanding and to apply of the ensuing findings for better planning and management of water resources in the basin.

Acknowledgements The authors would like to thank the RIMES (Regional Integrated Multi hazard Early Warning Systems) for providing their data on rainfall and discharge through their project on "Development and Implementation of User-Relevant End-to-End Flood Forecast Generation and Application System for Myanmar" to the first author during his internship at RIMES. Special thanks to the Director General of DMH, Myanmar, Dr. Anshul Agarwal (senior hydrologist, RIMES), and Dr. Pooja Sancheti for their support.

References

ADB (2009) is a report of ADB. Accessed from https://www.adb.org/sites/default/files/publication/27531/building-climate-resilience-agriculture-sector.pdf

Aryal A, Shrestha S, Babel MS (2018) Quantifying the sources of uncertainty in an ensemble of hydrological climate-impact projections. Theor Appl Climatol:1–17

Boori MS, Choudhary K, Evers M, Paringer R (2017) A review of food security and flood risk dynamics in central dry zone area of Myanmar. Procedia Eng 201:231–238

Brakenridge G, Syvitski J, Niebuhr E, Overeem I, Higgins S, Kettner A, Prades L (2017) Design with nature: causation and avoidance of catastrophic flooding, Myanmar. Earth-Sci Rev 165:81–109

Charan Pattnayak K, Kar SC, Kumari Pattnayak R (2015) Projections of rainfall and surface temperature from CMIP5 models under RCP4. 5 and 8.5 over BIMSTEC countries. In EGU general assembly conference abstracts(Vol. 17). Accessed from http://meetingorganizer.copernicus.org/EGU2015/EGU2015-556.pdf

Davies R (2018) is the reference for online news article from "floodlist" titled Myanmar-Deadly Floods and Landslides Strike Mohnyin District, Kachin State. Accessed from http://floodlist.com/asia/myanmar-floods-landslides-strike-kachin-state-june-2018

Defourney P, Vancutsem C, Bicheron P, Brockmann C, Nino F, Schouten L, Leroy M (2006) GLOBCOVER: a 300 m global land cover product for 2005 using Envisat MERIS time series. In Proceedings of the ISPRS commission VII mid-term symposium: remote sensing: from pixels to processes. Accessed from http://citeseerx.ist.psu.edu/viewdoc/download?doi=10.1.1.116.1909&rep=rep1&type=pdf

Easterling DR, Meehl GA, Parmesan C, Changnon SA, Karl TR, Mearns LO (2000) Climate extremes: observations, modeling, and impacts. Science 289:2068–2074

Endo N, Matsumoto J, Lwin T (2009) Trends in precipitation extremes over Southeast Asia. Sola 5:168–171

FAO (2016) is a report of FAO Aquastat. Accessed from http://www.fao.org/nr/water/aquastat/countries_regions/MMR/MMR-CP_eng.pdf

Garba H, Ismail A, Tsoho U (2013) Fitting probability distribution functions to discharge variability of Kaduna River. Int J Mod Eng Res 3:2848–2852

Ghimire U (2016) Analysis of historical and future climatic and hydrologic extremes in the Upper Ayerawaddy River Basin in Myanmarth. Asian Institute of Technology, Pathumthani

Gosain AK, Rao S, Basuray D (2006) Climate change impact assessment on hydrology of Indian river basins. Current science, 90(3), pp.346–353. Accessed from https://www.researchgate.net/profile/Ashvani_Gosain/publication/237268322_Climate_Change_Impact_Assessment_on_Hydrology_of_Indian_River_Basins/links/00b4953bd6fce3a881000000

Gudmundsson L, Bremnes J, Haugen J, Engen-Skaugen T (2012) Downscaling RCM precipitation to the station scale using statistical transformations–a comparison of methods. Hydrol Earth Syst Sci 16:3383–3390

Horton R, De Mel M, Peters D, Lesk C, Bartlett R, Helsingen H, Bader D, Capizzi P, Martin S, Rosenzweig C (2016) is a technical report on "Assessing the Climate Risk of Myanmar". Accessed from https://themimu.info/sites/themimu.info/files/documents/Report_Assessing_Climate_Risk_in_Myanmar_-_Technical_Report_Mar2017.pdf

Htway O, Matsumoto J (2011) Climatological onset dates of summer monsoon over Myanmar. Int J Climatol 31: 382–393

IPCC (2014) Climate Change 2014 – Impacts, Adaptation and Vulnerability: Part B: Regional Aspects: Working Group II Contribution to the IPCC Fifth Assessment Report. Cambridge: Cambridge University Press. https://doi.org/10.1017/CBO9781107415386

IWMI (2019) is based on an online webpage of IWMI CGIAR. Accessed from http://www.iwmi.cgiar.org/where-we-work/asia/southeast-asia/myanmar/key-water-issues/

Kar AK, Winn LL, Lohani A, Goel N (2011) Soft computing–based workable flood forecasting model for Ayeyarwady River Basin of Myanmar. J Hydrol Eng 17:807–822

Kattelus M, Rahaman MM, Varis O (2015) Hydropower development in Myanmar and its implications on regional energy cooperation. Int J Sustain Soc 7:42–66

Kay A, Davies H, Bell V, Jones R (2009) Comparison of uncertainty sources for climate change impacts: flood frequency in England. Clim Chang 92:41–63

Kendall MG (1948) Rank correlation methods. Oxford, England: Griffin

Khaing M (2015) Assessing Climate Change Impacts on Hydropower Generation in the Myitnge River Basin, Myanmar. Conference paper presented during Hydropower 2015 conference. Accessed from http://www.ich.no/Opplastet/Dokumenter/Hydropower15/khaing_myanmar.pdf

Krause P, Boyle D, Bäse F (2005) Comparison of different efficiency criteria for hydrological model assessment. Adv Geosci 5:89–97

Kreft S, Eckstein D, Junghans L, Kerestan C, Hagen U (2014) is a briefing paper of Global Climate Risk Index. Accessed from http://www.indiaenvironmentportal.org.in/files/file/global%20climate%20risk%20index%202015.pdf

Krysanova V, Vetter T, Eisner S, Huang S, Pechlivanidis I, Strauch M, Gelfan A, Kumar R, Aich V, Arheimer B (2017) Intercomparison of regional-scale hydrological models and climate change impacts projected for 12 large river basins worldwide—a synthesis. Environ Res Lett 12:105002

Lehner B, Verdin K, Jarvis A (2006) HydroSHEDS technical documentation, version 1.0. World Wildlife Fund US, Washington, DC, pp 1–27

Mann HB (1945) Nonparametric tests against trend. Econometrica: Journal of the Econometric Society, pp.245–259. https://doi.org/10.2307/1907187, https://www.jstor.org/stable/1907187

Maraun D (2013) Bias correction, quantile mapping, and downscaling: revisiting the inflation issue. J Clim 26: 2137–2143

Mendelsohn R, Dinar A, Williams L (2006) The distributional impact of climate change on rich and poor countries. Environ Dev Econ 11:159–178
Moriasi DN, Arnold JG, Van Liew MW, Bingner RL, Harmel RD, Veith TL (2007) Model evaluation guidelines for systematic quantification of accuracy in watershed simulations. Trans ASABE 50:885–900
Nan Y, Bao-hui M, Chun-kun L (2011) Impact analysis of climate change on water resources. Procedia Eng 24: 643–648
O'Gorman PA (2015) Precipitation extremes under climate change. Curr Clim Change Rep 1:49–59
Prudhomme C, Davies H (2009) Assessing uncertainties in climate change impact analyses on the river flow regimes in the UK. Part 2: future climate. Clim Chang 93:197–222
Sein K, Chidthaisong A, Oo K (2018) Observed trends and changes in temperature and precipitation extreme indices over Myanmar. Atmosphere 9:477
Sen PK (1968) Estimates of the regression coefficient based on Kendall's tau. J Am Stat Assoc 63:1379–1389
Shrestha S, Htut AY (2016) Land use and climate change impacts on the hydrology of the Bago River basin, Myanmar. Environ Model Assess 21:819–833
Shrestha B, Babel M, Maskey S, Van Griensven A, Uhlenbrook S, Green A, Akkharath I (2013) Impact of climate change on sediment yield in the Mekong River basin: a case study of the Nam Ou basin, Lao PDR. Hydrol Earth Syst Sci 17(1)
Soe MK (2018) is an online web news article. Accessed from http://www.globalnewlightofmyanmar.com/utilization-water-resources-myanmar/
Sok K, Oeurng C (2016) Application of HEC-HMS model to assess streamflow and water resources availability in Stung Sangker catchment of Mekong'Tonle Sap lake basin in Cambodia. https://doi.org/10.20944/preprints201612.0136.v1, Accessed from https://www.preprints.org/manuscript/201612.0136/v1
Sun X, Mein R, Keenan T, Elliott J (2000) Flood estimation using radar and raingauge data. J Hydrol 239:4–18
Tebaldi C, Hayhoe K, Arblaster JM, Meehl GA (2006) Going to the extremes. Clim Chang 79:185–211
Van Ty T, Sunada K, Ichikawa Y, Oishi S (2012) Scenario-based impact assessment of land use/cover and climate changes on water resources and demand: a case study in the Srepok River Basin, Vietnam—Cambodia. Water Resour Manag 26:1387–1407
Vetter T, Reinhardt J, Flörke M, van Griensven A, Hattermann F, Huang S, Koch H, Pechlivanidis IG, Plötner S, Seidou O (2017) Evaluation of sources of uncertainty in projected hydrological changes under climate change in 12 large-scale river basins. Clim Chang 141:419–433
WEPA (2005) is an online webpage of WEPA. Accessed from http://www.wepa-db.net/policies/state/myanmar/myanmar.htm
Wilby RL, Harris I (2006) A framework for assessing uncertainties in climate change impacts: Low-flow scenarios for the River Thames, UK. Water Resour Res 42
Yazid M (2015) Regional observed trends in daily rainfall indices of extremes over the Indochina Peninsula from 1960 to 2007. Climate 3:168–192
Yue S, Ouarda T, Bobée B, Legendre P, Bruneau P (1999) The Gumbel mixed model for flood frequency analysis. J Hydrol 226:88–100

Publisher's note Springer Nature remains neutral with regard to jurisdictional claims in published maps and institutional affiliations.

Affiliations

Uttam Ghimire[1,2] **· Mukand S. Babel**[1] **· Sangam Shrestha**[1] **· Govindarajalu Srinivasan**[2]

[1] Department of Water Engineering and Management, Asian Institute of Technology, Khlong Nueng, Pathumthani 12120, Thailand

[2] Regional Integrated Multi-Hazard Early Warning System for Africa and Asia (RIMES), Khlong Nueng, Pathumthani 12120, Thailand